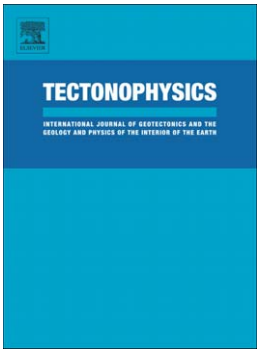

Fault and fracture patterns in low porosity chalk and their potential influence on sub-surface fluid flow – A case study from Flamborough Head, UK

D.A. Sagi, N. DE Paola, K.J.W. Mccaffrey, R.E. Holdsworth

PII: S0040-1951(16)30261-X
DOI: doi: 10.1016/j.tecto.2016.07.009
Reference: TECTO 127184

To appear in: *Tectonophysics*

Received date: 13 December 2015
Revised date: 3 July 2016
Accepted date: 15 July 2016

Please cite this article as: Sagi, D.A., DE Paola, N., Mccaffrey, K.J.W., Holdsworth, R.E., Fault and fracture patterns in low porosity chalk and their potential influence on sub-surface fluid flow – A case study from Flamborough Head, UK, *Tectonophysics* (2016), doi: 10.1016/j.tecto.2016.07.009

Fault and fracture patterns in low porosity chalk and their potential influence on sub-surface fluid flow – A case study from Flamborough Head, UK

D. A. SAGI*[1, 2], N. DE PAOLA[1], K. J. W. MCCAFFREY[1], and R. E. HOLDSWORTH[1]

[1]Rock Mechanics Laboratory, Earth Sciences Department, Durham University, South Road DH1 3LE, UK

[2]Currently at: Getech, Kitson House, Elmete Hall, Elmete Lane, Leeds, LS8 2LJ, UK

*Corresponding author: Tel: +441133222231 e-mail: david.sagi@getech.com

Abstract

To better understand fault zone architecture and fluid flow in mesoscale fault zones, we studied normal faults in chalks with displacements up to 20 m, at two representative localities in Flamborough Head (UK). At the first locality, chalk contains cm-thick, interlayered marl horizons, whereas at the second locality marl horizons were largely absent. Cm-scale displacement faults at both localities display ramp-flat geometries. Mesoscale fault patterns in the marl-free chalk, including a larger displacement fault (20 m) containing multiple fault strands, show widespread evidence of hydraulically-brecciated rocks, whereas clays smears along fault planes, and injected into open fractures, and a simpler fault zone architecture is observed where marl horizons are present. Hydraulic brecciation and veins observed in the marl-free chalk units suggest that mesoscale fault patterns acted as localized fault conduit allowing for widespread fluid flow. On the other hand, mesoscale fault patterns developed in highly fractured chalk, which contains interlayered marl horizons can act as localized barriers to fluid flow, due to the sealing effect of clays smears along fault planes and introduced into open fractures in the damage zone.

To support our field observations, quantitative analyses carried out on the large faults suggest a simple fault zone in the chalk with marl units with fracture density/connectivity

decreasing towards the protolith. Where marls are absent, density is high throughout the fault zone, while connectivity is high only in domains nearest the fault core.

We suggest that fluid flow in fractured chalk is especially influenced by the presence of marls. When present, it can smear onto fault planes, forming localised barriers. Fluid flow along relatively large displacement faults is additionally controlled by the complexity of the fault zone, especially the size/geometry of weakly and intensely connected damage zone domains.

1. Introduction

According to classical fault zone models (e.g. Chester et al. 1993, Caine et al. 1996) natural fault zones are thought to comprise three main domains: 1) a *fault core* with single or multiple strands of fine- to ultra-fine grained fault rocks (e.g. gouges, cataclasites), where most of the slip is localised; 2) a *damage zone* of fractured and brecciated rocks, where the intensity of the fracturing progressively decreases as one moves away from the fault core; and 3) the *protolith* surrounding the fault core and the damage zone, made of intact host rock, where the effects of fault-related deformation are minor or absent. The geometry, thickness, type of fault rocks and development of fault/fracture patterns in the fault core and damage zone are strongly influenced by the lithology of the host rocks (e.g. Caine et al. 1996; Agosta et al. 2007, Antonellini & Aydin 1994, De Paola et al. 2008, Faulkner et al. 2003).

Previous studies (e.g. Chester et al., 1993, Sagi et al., 2013,) show that fracture density and connectivity monotonically decreases in the damage zone of faults developed in a wide range of lithologies. However, it has been also suggested that fracture density and connectivity vary in a more complex fashion across the damage zone of carbonate-hosted fault zones (e.g. Billi et al., 2003). In particular, Micarelli et al. (2003, 2006a, 2006b) recognised distinct weakly deformed (WDDZ) and intensely deformed (IDDZ) damage zone domains, based on the observed variations of fracture density in fault zones hosted in low-porosity carbonates. According to their observations, the IDDZ is located closer to the fault

core, and it is characterised by higher fracture density values than the WDDZ, which is located further away from the fault core, and the boundary between the two domains is sharp.

The nature and distribution of fault rocks and fracture pattern domains in fault zones are lithology-dependent, and control the fault zones transport properties (Antonellini and Aydin, 1994; Caine et al., 1996; Chester and Chester, 1998; Chester et al., 1993; Collettini et al., 2009; De Paola et al., 2008; Faulkner et al., 2003; Lockner and Beeler, 1999; Seront et al., 1998, McQuillan, 1973). Fault zone fluid transmissibility can vary significantly within the different fault zone domains (e.g. Caine et al., 1996), and is primarily controlled by the distribution of associated fault rocks, facture connectivity (Odling, 1992) and orientation distribution (Sleight, 2001) of fractures within the different fault zone domains (e.g. Billi et al., 2003).

Specific sets of faults and associated fractures may strongly influence fluid migration in the upper crust (Caine et al., 1996; Sibson, 2000). Fluids may be preferentially transmitted along fault-parallel fracture corridors acting as conduits, as well as being retarded across faults acting as barriers (Evans et al., 1997). In this latter case, brittle cataclasis, which causes grain size reduction and slip localization in the fault core, can reduce the overall porosity and permeability (Antonellini et al., 1994; Byerlee, 1993).

Chalk is a generally fine grained carbonate rock characterised by a range of porosities (5-20%) and low permeability ($< 4*10^{-20}$ m^2), and it can act as an effective seal for hydrocarbons in the subsurface (Mallon et al., 2005). However, once fractured, chalk can develop significant amounts of structural porosity and may become highly permeable, up to 10^{-12} m^2 (e.g. Frykman, 2001; Scholle, 1977). The faults and associated fracture patterns developed within chalks are known to exhibit a great variability in fault attributes such as fracture density and connectivity (e.g. Agosta and Aydin, 2006; Aydin, 2000; Tondi, 2007). These variations have important applications for the hydrocarbon industry, as some of the

largest oil reservoirs in the North Sea (for example) occur in fractured chalk (e.g. the Ekofisk, Dan and Skjold Fields). Heavily fractured chalk is generally considered to be a good reservoir rock, based on structural porosity measurements showing values up to 30% (e.g. Odling, 1999, Egeberg and Saigal, 1991). Chalk reservoirs also have a strategic role, as they are potential target sites for sub-surface CO_2 sequestration and storage (Wilson et al., 2007). Finally, chalk reservoirs in onshore regions adjacent to the North Sea, form potentially important strategic aquifers for water suppliers, for example in East Yorkshire (Price, 1987).

In this paper, a case study of a reservoir field analogue from coastal exposures of faulted and fractured chalk at Flamborough Head, Yorkshire, is presented. The studied outcrops are representative of sub-surface chalk reservoirs in the nearby onshore and offshore regions in North Sea. The architecture and geometry of small (cm-scale offsets) and relatively large displacement faults (offsets up to a few tens of meters) are described, and the fracture, vein density and connectivity of the associated fracture/vein networks are characterized. Field and microstructural observations on fault patterns developed in different lithological host rocks, at a range of scales, are integrated with quantitative analyses of fracture/vein density and connectivity, collected across the studied fault zones using 1D transect and 2D image analysis methods. On the basis of this study, we propose a conceptual model describing the potential influence of lithology-controlled fault and fracture patterns on subsurface fluid flow in fractured chalk reservoirs.

2. Geological setting and study areas

Flamborough Head forms part of the Yorkshire coast in the UK (Fig. 1a), located north of Bridlington, at the eastern termination of the E-W trending, extensional Howardian-Flamborough Fault Belt (Fig. 1b). This fault-belt forms the southern boundary of the partially inverted Mesozoic Cleveland Basin and the northern boundary of the Market Weighton Block (Hawkins and Aldrick, 1994; Kirby and Swallow, 1987). The Howardian-Flamborough Fault

Belt was initially formed as a set of normal faults during the Late Jurassic–Early Cretaceous, and was later reactivated as a network of reverse faults/thrusts during the Late Cretaceous and Early Cenozoic (Kirby and Swallow, 1987).

The southern termination of the approximately coast-parallel Peak Trough Fault System is also located close to Flamborough Head (Fig. 1b). The Peak Trough is a N–S-trending, extensional, Jurassic fault system. Similarly to the Howardian-Flamborough Fault Belt, the Peak Trough Fault System was also reactivated during the Cenozoic during the inversion of the Cleveland Basin (Milsom and Rawson, 1989).

Thus the fault patterns in the Flamborough Head area result from of a series of deformation events, including both N-S oriented extension (Late Jurassic-Early Cretaceous) and E-W oriented (Cenozoic) shortening. At Flamborough Head, fault patterns are complex due to its location close to the intersection of the Howardian-Flamborough Belt and the Peak Trough fault systems.

The well-exposed cliff sections at Flamborough Head make it particularly suitable for studying faults and associated fracture systems in chalk. First studied geologically by Lamplugh (1895), the high (>20 m) cliffs and foreshore are made up entirely of well-stratified Upper Cretaceous chalk. These fine-grained, low porosity, homogenous beds are between 2 mm and 1.5 m thick (Childs et al., 1996) and are locally interlayered with 1-80 mm thick, clay-rich, marly horizons (Lamplugh, 1895).

Outcrop-scale, field-based structural observations and microscale diagenetic studies suggest that, after burial to a depth of about 0.8-1.5 km during the Early Cenozoic (Hillis, 1995; Stewart and Bailey, 1996), the chalk experienced several phases of deformation, producing a wide range of deformation features (e.g. Childs et al., 1996; Starmer, 1995). Based on preferential cross-cutting relationships and fault orientations, Peacock & Sanderson (1994) suggested that the small (cm-scale) displacement normal faults, which are exposed at

Flamborough Head developed in an extensional paleostress field, with σ_1 oriented sub-vertical, and the far-field σ_3 interpreted to have been approximately N-S oriented with a magnitude close to the E-W oriented σ_2. As a result, the stress release on the large normal faults caused switching between the approximately equal horizontal paleostresses in the areas between the large faults, resulting in the development of complex, mutually orthogonal mesoscale fault patterns, accommodating approximately 1% extension in all horizontal directions (Peacock & Sanderson, 1994). Starmer (1995) also interpreted the small displacement normal faults at Flamborough Head as having developed in a stress field characterized by isotropic horizontal stresses during the Late Cretaceous–Palaeocene.

Peacock and Sanderson (1994) observed that the characteristic ramp-flat geometries, which were developed in association with the small displacement normal faults, are lithologically controlled by the presence of marly horizons that are interlayered within the chalk beds in some areas. Additionally, Childs et al. (1996) showed that the vertical displacements of the small displacement normal faults, across adjacent chalk beds, can be controlled by the presence of marl-rich layers, producing a range of different fault geometries, including contractional and extensional jogs, overlaps and bends.

The present study focuses on two locations, where detailed structural observations have been collected and integrated with 1D and 2D quantitative datasets: Selwick Bay and Dykes End (Fig. 1c). These localities were selected based on the quality of the exposures that best represent the main faulting styles and relationships in the region. At Dykes End, the cliffs can be studied over a length of several kilometres, while at Selwick Bay, the cliffs and foreshore sections are exposed for several hundred meters and are extensively incised, providing good 3D exposures of the preserved structures.

At Selwick Bay, which exposes rocks stratigraphically lower in the sequences compared to Dykes End, two large displacement (up to 20 m combined displacement, Lamplough, 1895),

ENE-WSW trending normal fault zones can be observed in the vertical cliff section and traced in plan view along the wave-cut platform. The two fault segments lie 4 m apart, trending sub-parallel to each other. At Dykes End, a NW-SE trending larger displacement normal fault zone with approximately 1 m offset was observed. At both locations, we studied the widespread brittle deformation manifest by many small displacement (up to a few cm) normal faults and associated fracture and vein patterns.

3. Structural Observations

3.1. The protolith

The Upper Cretaceous chalk at Flamborough Head is well-bedded with an average bed thickness of approximately 25 cm. At Dykes End, the chalk beds are in places interlayered with clay-rich, marl horizons that have a thickness ranging from a few mm up to ~5 cm, and their combined thickness makes up approximately 5% of the total outcrop volume (Fig. 2a). By contrast, at Selwick Bay, interlayered marl horizons are rare (< 1% by volume) and, when present, have a maximum thickness of 2 mm (Fig. 2b). Bedding-parallel stylolites are common features at Selwick Bay, but they are rare at Dykes End (Fig. 2a-b). Closer to the larger displacement faults, a few sub-vertical to inclined stylolites can also be found at Selwick Bay. Clay-rich, mm-thick films of residual material are commonly observed on stylolitic surfaces (Fig. 2b).

Optical microscope observations of thin sections cut from the protolith show that the chalk matrix is very fine grained (Fig. 2c); the individual grains cannot be resolved even under 50x magnification. Brighter, circular or ellipsoidal zones, with sizes ranging from 10 to 100 μm, have been observed (Fig. 2c) and appear to be randomly dispersed in the matrix, although they occasionally show a preferential alignment. These brighter spots may represent recrystallized regions of chalk. Scanning electron microscope (SEM) images of thin sections show that the matrix is very homogenous, comprising grains with an average size of 50

microns in diameter (Fig. 2d). The individual grains do not appear to contain any intragranular fractures.

3.2. Small displacement normal faults

Selwick Bay

Small normal fault displacements range from 1 mm to 20 cm, and their orientation is scattered (Fig. 3a) with one major set of NW-SE striking fractures dipping at an angle greater than 70° (Fig. 3a). Kinematic indicators on the fault planes are rarely observed, and the few slickenlines observed show dip-slip to slightly oblique slip kinematics (Fig. 3a). At Selwick Bay, small displacement faults are often organized into conjugate sets, where individual segments mutually crosscut (Fig. 3b-c). The faults are often characterized by ramp-flat geometries (Fig. 3c-d) resulting in the development of dilational and compressional jogs, related to the ramp and flat sections, respectively.

Flat sections of the small displacement normal faults are often located on bedding planes. These bedding surfaces are also reactivated as stylolitic surfaces due to pressure solution (Fig. 3c-d). Dilational jog structures along the faults are almost always (>90%) filled with crystalline calcite (Fig. 3d). The widths of the jogs are up to 30 cm, and the individual calcite crystals within the jogs can grow up to 5 cm in length. Angular chalk clasts are in places found within calcite veins, and are up to 2-3 cm long. Compressional jogs are usually characterized by pressure solution features (Fig 3d), with thin films of residual, clay-rich material present on the stylolite surfaces.

The small displacement normal faults can also be observed in plan view, on the wave-cut platform in front of the cliffs. They are made of a braided, up to 0.5 m wide zones of veining, terminating by a series of en-echelon, calcite filled fractures (Fig. 3e). These geometries are very similar to those seen in the “zebra rocks” described by Holland and Urai (2010) in low porosity limestones in Oman. Most individual veins have an average thickness of 1-2 mm,

but the thickest can (locally) reach widths of up to 30 cm, and show clear evidence for hydraulic brecciation processes, with white angular wall-rock clasts dispersed in a crystalline calcite matrix (Fig. 3f). These textures are thought to form due to the hydraulic brecciation of the host rock, followed by a rapid drop in fluid pressure, which causes instantaneous calcite precipitation (Sibson, 2000). In most of the thin veins, the individual calcite crystals cannot be seen with the naked eye, but in the thickest veins they can grow up to 6 cm in length. The orientations of the crystals within the veins cannot be clearly observed in the field, due to weathering, to discriminate whether the veins formed as hybrid shear/extensional or pure tensile features.

Dykes End

The orientation of small displacement normal faults at Dykes End is scattered (Fig. 4a), with one major fault set striking NW-SE. The displacements range from 1 mm to 20 cm. Many of the fractures show smearing of marls layers onto the fault plane (Fig. 4b-c, see text below), and lack kinematic indicators. The few faults with observable slickenlines suggest dip-slip to slightly oblique slip, normal kinematics (Fig. 4a).

Most of the small displacement normal faults are characterised by ramp-flat geometries (Fig. 4b). The ramp sections are mostly located in the chalk beds, while the flat sections follow the interlayered marl horizons (Fig. 4b) that represent mechanically weak layers. Dilational jogs, developed along the ramp sections, are either open features, or (partially) filled with clay-rich materials, due to injection and smearing of material from the interlayered marl horizons (Fig. 4c). Compressional jogs, related to the flat sections of the faults, are characterized by intense, local fracturing of the chalk in the hanging wall, with the fractures generally organized in a radial pattern (Fig. 4d-e). There were no veins or other deformation features found at Dykes End that would suggest fluid assisted faulting and fracturing processes.

3.3. Large displacement normal faults

Selwick Bay

Two large displacement normal faults have been observed at Selwick Bay, both striking ENE-WSW, and dipping steeply (>70°) to the NNW (Fig. 5). The fault zones together form a promontory on the cliffs (Fig. 5a). The faults are located about 4 meters apart, diverging from each other slightly across the foreshore, towards the NE. The north facing fault has a well-defined fault core (hereafter referred to as the FC) characterized by a slip surface, located within a narrow (up to 10 cm) domain of fault gouge (Fig. 5a-b), whilst the south facing fault, instead of a fault core, is characterized by an intensely brecciated zone in its centre (hereafter referred as the IBZ), without a well-defined slip surface (Fig. 5a, c). The two faults are surrounded by damage zones that are 4-5 m wide in the footwall, but less than 1 m wide in the hanging wall. The damage zones are characterized by a higher density of calcite veins compared to the surrounding wall rocks.

In the hanging wall of the FC, the beds are almost vertical, possibly due to the along the fault (Fig. 5a-b). Calcite veins are less common in this region compared to the nearby cliff sections. The sub-vertical beds in the hanging wall are in direct contact with the FC which comprises two distinct domains: a) a sharp, narrow (10-15 cm) slip zone made of fault gouge with dispersed, small (cm-scale) clasts of the original host rock, bounded by a straight slip surface with slickenlines indicating dip-slip kinematics (Fig. 5b); b) an approximately 0.5-1 m wide zone of highly brecciated chalk, which exhibits a transitional boundary with the damage zone that separates the FC and IBZ. The IBZ is more than 1 m thick, and lacks a well-defined slip surface (Fig. 5c). The intensity of veining and calcite precipitation in the IBZ is higher than in the surrounding damage zone.

The damage zone between the FC and IBZ is characterized by tensile veining in the chalk, organized in a pervasive braided veining system. Widespread evidence for hydraulic

brecciation is shown by 2-3 cm large chalk angular clasts embedded within a calcite cement (Fig. 5c). Open fractures are rare, forming less than 5% of all fractures. The geometry and calcite fill within the veins are similar to those observed along the small displacement faults at Selwick Bay (Fig. 3c-d, Fig. 5d). Thicker veins have coarse grained crystals that can grow up to 5 cm, and are sometimes characterized by either a well-defined median line in the centre, or by the development of vuggy textures and cavities. Most of these large veins and vuggy fills locally crosscut the typically braided, smaller veins, perhaps suggesting a later origin when the fault was at shallow depths within the vadose zone. The damage zone in the footwall of the IBZ is also characterized by intense veining and fracturing, which gradually decreases when moving towards the protolith.

Thin sections have been obtained from rock samples collected along a fault-orthogonal transect from the different fault zone domains (Fig. 5f and 6a) to study the main microstructural features of the vein system (Fig. 6). Sample S3, from the brecciated part of the FC close to the slip surface, contains several interconnected anastomosing veins with thicknesses ranging from 0.5 mm to 7 mm (Fig. 6b-c). Sample S4, collected from the IBZ, contains fewer, thinner veins than S3 (Fig. 6a, d-e). The average width of the veins here is around 1 mm, and the average crystal size of the calcite cement is around 0.5 mm. In this sample, two major vein zones are seen to mutually cross-cut each other (Fig. 6d-e). Finally, sample S6 collected 4 m away from the fault core, in the hanging wall, shows only a few veins oriented sub-parallel to each other which do not intersect (Fig. 6a, f-g). In this case the connectivity is low compared to both previous samples described.

Overall, the samples from the FC (sample S3) and the IBZ (sample S4) contain veins that branch out with an anastomosing, braided geometry, forming fan shapes, which are similar to the veins observed associated with the small displacement normal faults in other parts of

Selwick Bay (e.g. Fig. 3c-f), and to the zebra rocks described by Holland and Urai (2009) in limestones, in Oman.

Dykes End

At Dykes End, a thoroughgoing fault with about 1 m displacement was observed (Fig. 7). The fault has an orientation of 169/50 NE, does not display a ramp-flat geometry, and is characterized by a well-developed fault core, where most of the displacement was accommodated (Fig. 7a). The fault core is continuous, and varies from 5 to 20 cm in thickness (Fig. 7b-c). It is mostly made of a clay-rich gouge, which developed from the smearing of the original marl horizons along the fault plane, and it contains cm-scale clasts of the original host rock (Fig. 7b-c). A localized slip surface displays well-developed dip-slip slickenlines (Fig. 7c).

Adjacent to the fault gouge, both in the hanging wall and the footwall, a 2-3 m wide zone of damage occurs, characterized by intense fracturing (Fig. 7a-b). Most of the fractures in the damage zone are open and a large proportion are sub-vertical (Fig. 7a-b). Some, particularly those closer to the fault core and/or to the interlayered marl horizons, are partially filled with clay, which appears to have been introduced into the fracture planes both by smearing and gravitational infilling. There was no field evidence found for veining or other fluid-assisted fracturing processes within the fault core and damage zone.

Microstructural observations from the different fault zone domains show that the fault gouge from within the fault core contains chalk clasts up to 4 mm in diameter (Fig. 8), dispersed in a very fine-grained matrix made of clay minerals and fine-grained chalk (sample F2, Fig. 8b-c; for sample location see Fig. 7d and 8a). The chalk clasts are slightly elongate, with rounded edges and are homogenously distributed in the matrix showing no preferred orientation (Fig. 8b-c). Thin sections cut from samples taken from the heavily fractured damage zone, 10 cm away from the core (sample D1 in Fig. 8a), show the presence of open

fractures (Fig. 8d-e). Some of these fractures formed due to the reactivation of stylolitic planes, which can be observed from the 2-3 mm long stylolite teeth (Fig. 8d-e). Optical microscope images from samples collected 20 cm away from the slip zone (sample D9 in Fig. 8a) show lower fracture densities (Fig. 8f-g).

4. Quantitative analysis of fracture density and connectivity in the fault zones of large displacement faults

Quantitative fault attribute data were collected across the large displacement normal faults at Selwick Bay and Dykes End along 1D line transects oriented at a high angle to the main fault trend, and from high resolution (6 Megapixel) outcrop scale and microscale photos by 2D image analysis.

4.1. 1D structural transect methods

Quantitative data were collected along sub-parallel transects, oriented at a high angle to the strike of the faults, located near to the cliffs and on the adjacent wave-cut platform (N1-N3 at Selwick Bay and N4-N5 at Dykes End, Fig. 5f, 7d). The transects ranged in length between 10 and 20 m, depending on the thickness of the damage zones. For each structural feature (e.g. fractures and veins) the distance along the transect, the strike, dip, dip direction, width and nature of the filling material were recorded. Where observed, the fault offset and the rakes were also recorded.

The N1 transect along the cliff face at Selwick Bay was irregular, with some sections oblique to the fault strike. In this case the fracture density data were corrected to account for the obliquity between the transect trend and the fault strike. The original transect was divided into three sections, each characterised by a specific acute angle oriented with respect to the fault strike (Fig. 5f). Fracture and vein density in 1D were defined as the number of features (n) per meter (n/m), and their values along each transect have been plotted in fracture density vs. distance along the transect graphs.

4.2. 2D image analysis methods

2D quantitative image analyses were performed on: a) high resolution digital photos, taken from the exposures of the large displacement normal faults with a constant camera-outcrop distance of 5 m, oriented parallel to the outcrop sections (Fig. 5f, 7d), and b) from thin sections obtained from samples collected from different fault zone domains along the N1 and N5 transects at Selwick Bay and Dykes End, respectively (Fig. 5f, 7d).

Mesoscale fractures, veins and bedding surfaces were digitized from outcrop photos (e.g. Figs. 11b and 13b.). Using a 5 m outcrop-camera distance and a 6 Megapixel camera the narrowest features that could be resolved were approximately 5 mm wide. For both outcrops each photo was divided into 3 different panels ("P"), each panel representing an approximately 1 m wide cliff section (Fig. 5f, 7d). The fracture and vein density was measured using the total length of fractures/veins within the sampling area (m/m^2). Connectivity was calculated using two different methods: a) intersection point density (IPD) as described by Odling (1992, 1997), expressed as n/m^2 (the number of intersection points within a unit area) and b) the fractional connected area (FCA) as described by Ghosh and Mitra (2009), expressed as a percentage (the summed area of all the clusters of interconnected fractures, divided by the total sample area). Our results show that the correlation between the two methods is high (R^2=0.90) and using an equation of IPD=0.95FCA-0.34 they can be used interchangeably for this specific dataset.

In addition to mesoscale structures, microfractures, stylolites and veins were digitised from accurate greyscale images obtained from digital scans of thin sections. These images were used to calculate 2D microscale fracture and vein density and connectivity using the same methods as described above.

4.3.1D transect results

Selwick Bay

The fractures associated with the large displacement normal faults at Selwick Bay are almost all calcite filled, i.e. veins (>90%). Vein density was calculated along three transects orthogonal to the fault zones (Fig. 9a, for transect locations see also Fig. 5f). Veins in the damage zone have a dominant trend, oriented parallel to the large faults, and they dip between 50° and sub-vertical (Fig. 9b). The few shear planes observed display slickenlines with dip-slip to oblique slip kinematics (Fig. 9b).

Based on measurements further away from the fault zone, the background density of veins was found to be approximately 2/m (Fig. 9c-e). The footwall damage zone of the IBZ is up to 3 m wide, beyond which the intensity of damage gradually decreases towards the background vein values (Fig. 9c-e). The vein density and damage zone width in the hanging wall to the FC are variable along the profiles (Fig. 9c-e), with up to 4 m wide damage zone (Fig. 9e). In between the FC and the IBZ, vein density is higher closer to both fault zones and decreases to background values within 2-3 m (Fig. 9c-e). The highest vein density values are measured where the distance between the IBZ and FC is smaller than their damage zones widths (Fig. 9c). The average vein width was also measured for each meter of the three transects, but these values do not show a clear systematic variation across the fault zones (Fig. 9f-h), although vein width seems to show a weak negative correlation with vein density (Fig. 9f-g).

Dykes End

The orientation of fractures in the damage zone of the large displacement normal fault at Dykes End is similar to that of the main fault itself (Fig. 10a). The fault and most of the fractures in the damage zone are oriented NW-SE, with dips greater than 60° (Fig. 10a). The few kinematic indicators, observable on the fracture planes within the damage zone of the large displacement normal fault suggest dip-slip to slightly oblique slip, normal kinematics (Fig. 10a).

Based on measurements further away from the fault zone, the background fracture density was estimated to be approximately 5/m. The damage zone is up to 3 m wide, with the intensity of damage decreasing away from the fault core. It displays an asymmetric distribution with higher fracture density values in the fault hanging wall (approximately 20/m) compared to the footwall (approximately 10/m, Fig. 10b-c).

Some fractures in the damage zone are filled with marls that have been introduced into the fracture planes from the interlayered horizons during/after fracture opening. The number of open fractures diminishes slightly closer to the fault core, where values, which are comparable to the background fracturing, are observed (except for the second meter on the N5 transect). Conversely, the density of clay-filled fractures is significantly higher in the near vicinity of the fault core, compared to the outer parts of the damage zone and the protolith (Fig. 10b-c).

4.4.2D Image analysis

Selwick Bay – outcrop scale analysis

In the case of Selwick Bay, five photos were taken to cover the entire exposure of the large displacement normal fault (Fig. 11a; Fig. 5f). Each image was divided into 3 panels, each representing an approximately 1 m long section of cliff. Vein density and connectivity were calculated within each panel (see Fig. 11b). Within each panels the veins and the bedding surfaces were marked with black lines and the FCA as a dark grey area.

The variation of vein density in 2D across the IBZ and FC at Selwick Bay is plotted on Fig. 11c. High vein density values define damage zones in the IBZ footwall (up to 4 wide), in the FC hanging wall (up to 3 m wide) and in between the FC and the IBZ (Fig. 11c). Vein density values in these domains are up to 4 times higher (4 m/m^2) than in the wall rocks where background values are approximately 1 m/m^2. In other sections of the damage zone (e.g. P1-3, P13-P15) density values are up 2 times higher (2 m/m^2) than the background

values. Vein connectivity results suggest that the damage zone can be divided into weakly deformed damage zones (WDDZ) and intensively deformed damage zones (IDDZ) sub-domains, following the convention introduced in Micarelli et al. (2005) for carbonate fault zones.

Vein connectivity values, measured as both FCA and IPD, vary across the fault zone in a similar fashion to vein density (Fig. 11d-e). However, their relative increase, when compared to background values, can be as high as one order of a magnitude (Fig. 11d-e). Panels, located in the footwall, close to the IBZ (P4-6), and between the FC and IBZ (P8-9) are characterized by FCA and IPD connectivity values between 50% and 80% and 70 n/m^2 and 120 n/m^2, respectively. Panels in the footwall (P1-3), and in the hanging wall of the FC (P13-15) are typically characterized by low FCA and IPD vein connectivity values, less than 10% and 20 n/m^2, respectively. Based on the variation of fracture connectivity, hereafter damage zone domains characterized by high (>40%) connectivity values will be referred to as intensively connected damage zones (ICDZ), and damage zone domains, characterized by low (<20%) connectivity values will be referred to as weakly connected damage zones (WCDZ).

The crossplot between vein density and connectivity data, calculated as FCA, shows that the datapoints group into two distinct clusters, fitted by a linear trend, defining the distinct domains with different connectivity (Fig. 11f). The weakly connected damage zone is characterised by moderate to high vein density and relatively low vein connectivity values, while the intensely connected damage zone has high vein density and high vein connectivity values. The latter domains are located in the region between the FC and the IBZ (P8-9) and in the footwall damage zone adjacent to the IBZ (P4-6); while the weakly connected domains (P1-3, P13-15) are located further away from the FC and IBZ.

Vein connectivity, as depicted on the IPD versus vein density cross-plot, shows somewhat different characteristics, compared to the FCA equivalent (Fig. 11g). The data are best fitted by a power-law trend, and show a more continuous distribution where the transition from the weakly to intensely connected domains is gradual (Fig. 11g).

Selwick Bay – microscale analysis

Vein density values have also been obtained by digital quantitative analysis performed on thin sections, collected from the different fault zone domains (for sample location see Fig. 5f). Vein density and connectivity were also measured at this scale in the IBZ and FC. The results show that the background fracture density in the protolith is approximately 200 m/m^2 (Fig 12a, data from S1 and S6 samples in Fig. 5f). This value is significantly lower than the values gained from thin sections collected from the damage zones, in the IBZ and in the FC. Vein densities in the fault zone range between 700-1000 m/m^2. The highest values are measured in the brecciated parts of the FC (S3 sample, 1000 m/m^2), and decreases gradually in the intensely connected part of the damage zone (S2 sample, 900 m/m^2), in the IBZ (S4 sample, 800 m/m^2) and, finally, the lowest values are measured in the weakly connected damage zone (S5 sample 700 m/m^2). The differences between the values measured from samples within the fault zone are not significant when compared to the increase observed with respect to the background values calculated for the protolith. Vein connectivity in the protolith was found to be low (<10%), compared to the damage zones and fault cores, where vein connectivity values range between 20% and 60% (Fig. 12b). In the FC and IBZ vein connectivity values are 50% and 40%, respectively; while in the damage zone vary from 60% and 20%, respectively.

The vein connectivity versus vein density cross-plots for the microscale results show a similar trend to that observed for the outcrop scale results (Fig. 12c). The protolith is characterized by low vein density, and low vein connectivity, the weakly connected damage

zone is characterized by high vein density, but relatively low vein connectivity and the IBZ, the brecciated parts of the FC and the intensely connected damage zone are all characterized by high vein density and vein connectivity values (Fig. 12c). A best fit, power-law trendline fitted to the data ($y=0.1101x^{5157}$, where y is vein density and x is vein connectivity, measured as FCA) is characterized by a relatively high R^2 value (0.77). The datapoints do not cluster as much as was the case for the outcrop scale results (Fig 11f). .

Dykes End

2D fracture density and connectivity data at the Dykes End large displacement normal fault was collected from 6 fault zone parallel panels, each approximately 1 m wide (Fig. 13a-b). In the damage zone to the large displacement normal fault, fracture density increases towards the fault core (Fig. 13c). In the footwall, fracture density values close to the fault core (3.5 m/m^2) are approximately 4 times higher than those measured outside the damage zone (< 1 m/m^2). Fracture density values in the footwall, close to the fault core (P3) are twice as high as in the hanging wall (2 m/m^2, P5).

Fracture connectivity across the damage zone, measured as FCA, also shows significantly higher values in the footwall damage zone (up to 60%) than in the hanging wall damage zone (up to 20%, Fig. 13d). Finally, fracture connectivity values, measured as IPD (Fig. 13e) also show higher values in the footwall (up to 90 n/m^2), than in the hanging wall (up to 40 n/m^2). The latter monotonically increases towards the fault core in contrast to those measured by FCA (Fig. 13d), where this effect was not observed.

Fracture density versus connectivity cross-plots, based on the data from Dykes End, show that fracture connectivity scales with fracture density (Fig. 13f-g), regardless of the method used to quantify connectivity. A linear best fit trendline is obtained when fracture connectivity is calculated by FCA (Fig. 13f), as opposed to a power-law best-fit obtained when connectivity is calculated as IPD (Fig. 13g).

5. Discussion

5.1. Lithological control on fault patterns and implications for fluid flow in fractured reservoirs

Based on the field observations and the qualitative data collected and analysed, a simple conceptual model of fluid flow is proposed, which can be applied to reservoirs hosted in fractured chalk similar to those seen at Flamborough Head.

Small displacement normal faults

The protolith at Dykes End is characterised by thick (cm-scale), interlayered marl horizons, whilst at Selwick Bay interlayered marl horizons are largely absent (Fig. 2a-b, 14a). Widespread, brittle deformation in both study areas is accommodated by patterns of small displacement normal faults with ramp-flat geometries (Fig. 3-4, 14b). At Dykes End, the interlayered, thick marl horizons are smeared out along the small displacement faults and are locally introduced into the associated fracture planes (Fig. 4b-c). Flat sections of the small displacement normal faults are associated with the presence of radial fractures and dilational step-overs. Small fractures further away from the small faults are open cracks with no filling material (Fig. 4d-e). No evidence for veining or other fluid assisted fracturing processes have been observed. Conversely, at Selwick Bay, most of the fractures associated with the small displacement normal faults are filled with crystalline calcite (Fig. 3c-f), suggesting fluid assisted fracturing processes (hydrofracturing) during deformation.

Thick (cm-scale) marl horizons, like the ones present at Dykes End, may act as effective barriers for fluids. The horizontal marl horizons can act as barriers to vertical fluid flow, while the marls smeared along faults and in steeply dipping fracture voids potentially act as good barriers for fluids migrating in other directions. Since the orientation distribution of the small displacement normal faults at Dykes End is very scattered (Fig. 4a), they may behave as distributed barriers, limiting horizontal fluid migration in all directions (Fig. 14b).

Conversely, at Selwick Bay, where small displacement normal faults are also characterized by scattered orientation (Fig. 3a), the fractures likely behave as distributed conduits, favouring the migration of fluids in all directions due to the absence of the interlayered marl horizons in the host rock (Fig. 14b).

Highly fractured chalk is usually considered to be a good reservoir rock, but our observations suggest that lithology plays a key role in controlling fluid flow, as the presence of thin marl layers can result in a highly compartmentalized, poor reservoir. Conversely marl-poor regions potentially provide a good reservoir, with distributed small displacement normal faults providing high structural porosity and permeability, enhancing reservoir fluid transmissibility (Fig. 14b).

Large displacement normal faults

In both study areas, deformation is localized along larger displacement normal faults (Fig. 5-8, Fig. 14c). At Dykes End, the large displacement normal fault comprises a narrow fault core with gouge, and an over 2 m wide damage zone surrounding the core, characterized by high fracture densities (Fig. 7). Many of the fractures in the damage zone are filled with marl introduced from the adjacent interlayered marl horizons (Fig. 7b-c). In the fault zone, no fluid assisted fracturing processes have been observed. Based on these observations, we suggest that large displacement normal faults of this kind are likely to behave as localised barriers to fluids (Fig. 14c).

At Selwick Bay, the large displacement normal faults are characterized by a more complex internal architecture, with heavily fractured damage zones (Fig. 5). The widespread mineralization provides extensive evidence for fluid assisted fracturing processes. The narrow layer of fault gouge observed on the slip surface in the FC (Fig. 5b), may have acted as a local barrier for fluids migrating across the fault core and could explain the absence of veins observed in the hanging wall damage zone of this fault. We suggest that overall,

however, the large displacement normal faults at Selwick Bay behaved as conduits, favouring the migration of fluids that were channelized into the fault zone. The vein connectivity data (Fig. 11d-e) suggests that fluid flow was mainly localized in into the footwall damage zone, the IBZ, the damage zone between the FC and IBZ and the most brecciated parts of the FC close to the fault core-hanging wall damage zone boundary.

5.2.The internal architecture of fault zones from 1D and 2D quantitative analysis: implications for fluid flow

At Dykes End, both 1D and 2D outcrop-scale quantitative analyses reveal a rather simple distribution of fracturing across the fault zone, with a gradual decrease in fracture density and connectivity within the damage zone, when moving from the fault core (Fig. 10, 13). According to the 1D results, the damage zone is asymmetric, being wider in the footwall (> 2 m) than in the hanging wall (< 1-2 m, Fig. 10). The relative increase in fracture density from the protolith to the damage zone near to the fault core is approximately 3-4 times. The increase is larger in the outer parts of the damage zone (up to 5/m) and smaller in the inner parts (1-2/m, Fig. 10b-c, 13c). Along the same sections, fracture connectivity only increases to double its background values (Fig. 13d-e). Similarly to the changes in fracture density, the increase is larger in the outer parts of the damage zone (up to 20%) and smaller in the inner parts (0-5%).

At Selwick Bay, a more complex picture emerges, with identification range of across-fault domains and sub-domains, characterized by a heterogeneous distribution of fracturing (Figs. 9, 11-12). 1D vein density data, collected along 3 sub-parallel structural transects, N1, N2 and N3 (Fig. 5f), were used to create a map of the distribution of vein density around the fault. Based on corresponding vein density and connectivity values along N1 transect and 2D image analysis, values less than 2/m were classified as protolith, rising to values larger than

4/m in the most intensely connected parts of the damage zone close to the fault core. Vein density values are higher in the zones where the two fault zone damage zones overlap.

Vein connectivity values rapidly increase, by over an order of magnitude, towards the inner parts of the damage zone. Following Micarelli et al. (2006b), the heterogeneous distribution of connectivity in the damage zone has been described in terms of intensely- and weakly connected damage zone sub-domains (Fig. 11f).

A conceptual model for the fault zone at Dykes End shows that the width of the damage zone and the amount of damage is similar in the footwall and in the hanging wall (Fig. 15a), however the damage zone width is somewhat larger in the hanging wall side, whereas fracture density and connectivity values are somewhat larger on the footwall side. Both fracture density and connectivity increases towards the fault core in a non-linear fashion, although not enough data was collected to determine the exact nature of this increase (i.e., exponential, power law, or an alternative model).

A conceptual model for the fault zone at Selwick Bay shows a much more complex fault zone architecture (Fig. 15b). Here, the development of the damage zone sub-domains may be explained by the partial overlap between the damage zones of two closely spaced, large displacement normal faults. In this situation, within the overlapping areas, the vein connectivity is high and this may also help to channelize fluids along the fault zone.

Both conceptual fault zone models show similar levels of damage near to the fault cores (Fig. 15a-b), with similar density and connectivity values even though the background fracturing values were different. This may be due to the fractures reaching a threshold of full connectivity.

Fracture/vein density and connectivity values can be normalised against the background values measured in the protolith in order to see the relative increase in damage in the different damage zone domains compared to the background fracturing (Fig 15c-d). Our results show

that in case of the Selwick Bay large displacement normal fault the weakly connected part of the damage zone is characterized by a 2-5 times increase in vein density, whereas the intensely connected part is characterized by an increase of 3.5-8 times depending on the method used (Fig. 15c). Vein connectivity values increase to approximately 2 times the protolith value in the weakly connected region rising to 7-14 times in the intensely connected part of the damage zone (Fig 15d).

6. Conclusions

Qualitative field observations and quantitative analyses of faults and fracture patterns in low porosity chalk at Flamborough Head show that:

(a) The fault rocks and fracture fills of small displacement normal faults is controlled by the protolith, in particular, by the presence of interlayered marl horizons. When thick (cm-scale) interlayered marl/clay-rich horizons are present in the protolith rocks, no fluid related mineralization features have been observed. Conversely, in protolith rocks lacking the interlayered marls/clay-rich horizons, abundant evidence of fluid assisted deformation (hydraulic fracturing) is widely preserved. These observations suggest that small displacement normal faults, developed in highly fractured chalk, which contains interlayered marl horizons can act as barriers to fluid flow, due to the sealing effect of clays smears along fault planes and introduced into open fractures in the damage zone. Conversely, small displacement normal faults developed in chalk lacking interlayered marl horizons can behave as conduits for fluid flow, especially within intensely fractured damage zones and within dilatant portions of the fault planes themselves (e.g. dilational jogs).

(b) In a predictable way, fracture density increases gradually from the protolith towards the fault core in the fault zone of the large displacement normal fault at Selwick Bay. However, vein connectivity has been observed to be much higher in the most inner parts of the damage zone, close to the fault core. As a result, the damage zone can be divided into two

distinct domains, an intensively connected damage zone, close to the fault core, and a weakly connected damage zone further away from it, towards the protolith rocks.

(c) High fracture density and connectivity domains are localized close to the fault cores, and where the damage zones of the large displacement normal faults overlap each other, These intensively connected damage zones are the domains where most fluids are channelized and can represent critical sites of interest during reservoir analyses.

7. Acknowledgement

The PhD studentship under which this paper was written is funded by MAERSK Oil, and additional funding for the fieldwork was provided by the AAPG, via the Norman H. Foster Memorial Grant, in the Grants-In-Aid programme.

8. Reference list

Aarland, R. K. & Skjerven, J. 1998. Fault and fracture characteristics of major fault zone in the North Sea: analyses of 3D seismic and oriented cores in the Brage Field (Block 31/4). In: Coward, M.P., Databan, T.S., Johnson, H. (Eds.). *Structural Geology in Reservoir Characterization* 127, 209-229.

Agosta, F., Prasad, M. & Aydin, A. 2007. Physical properties of carbonate fault rocks, fucino basin (Central Italy): implications for fault seal in platform carbonates. *Geofluids* 7, 19-32.

Agosta, F. & Aydin, A. 2006. Architecture and deformation mechanism of a basin-bounding normal fault in Mesozoic platform carbonates, central Italy. *Journal of Structural Geology* 28(8), 1445-1467.

Antonellini, M. & Aydin, A. 1994. Effect of faulting on fluid-flow i nporous sandstones - Petrophysical properties. *Aapg Bulletin-American Association of Petroleum Geologists* 78(3), 355-377.

Aydin, A. 2000. Fractures, faults, and hydrocarbon entrapment, migration and flow. *Marine and Petroleum Geology* 17(7), 797-814.

Billi, A., Salvini, F., Storti, F. 2003. The damage zone-fault core transition in carbonate rocks: implications for fault growth, structure and permeability. *Journal of Structural Geology* 25, 1779-1794.

Berg, S. S. & Skar, T. 2005. Controls on damage zone asymmetry of a normal fault zone: outcrop analyses of a segment of the Moab fault, SE Utah. *Journal of Structural Geology* 27(10), 1803-1822.

Byerlee, J. 1993. Model for episodic flow of high-pressure water in fault zones before earthquakes. *Geology* 21(4), 303-306.

Caine, J. S., Evans, J. P. & Forster, C. B. 1996. Fault zone architecture and permeability structure. *Geology* 24(11), 1025-1028.

Chester, F. M. & Chester, J. S. 1998. Ultracataclasite structure and friction processes of the Punchbowl fault, San Andreas system, California. *Tectonophysics* 295(1-2), 199-221.

Chester, F. M., Evans, J. P. & Biegel, R. L. 1993. INternal structure and weakening mechanisms of the San-Andreas Fault. *Journal of Geophysical Research-Solid Earth* 98(B1), 771-786.

Childs, C., Nicol, A., Walsh, J. J. & Watterson, J. 1996. Growth of vertically segmented normal faults. *Journal of Structural Geology* 18(12), 1389-1397.

Collettini, C., De Paola, N. & Faulkner, D. R. 2009. Insights on the geometry and mechanics of the Umbria-Marche earthquakes (Central Italy) from the integration of field and laboratory data. *Tectonophysics* 476(1-2), 99-109.

De Paola, N., Collettini, C., Faulkner, D. R. & Trippetta, F. 2008. Fault zone architecture and deformation processes within evaporitic rocks in the upper crust. *Tectonics* 27(4), 21.

Evans, J. P., Forster, C. B. & Goddard, J. V. 1997. Permeability of fault-related rocks, and implications for hydraulic structure of fault zones. *Journal of Structural Geology* 19(11), 1393-1404.

Faulkner, D. R., Lewis, A. C. & Rutter, E. H. 2003. On the internal structure and mechanics of large strike-slip fault zones: field observations of the Carboneras fault in southeastern Spain. *Tectonophysics* 367(3-4), 235-251.

Frykman, P. 2001. Spatial variability in petrophysical properties in Upper Maastrichtian chalk outcrops at Stevns Klint, Denmark. *Marine and Petroleum Geology* 18(10), 1041-1062.

Ghosh, K. & Mitra, S. 2009. Two-dimensional simulation of controls of fracture parameters on fracture connectivity. *Aapg Bulletin* 93(11), 1517-1533.

Hawkins, T. R. W. & Aldrick, R. J. 1994. The pattern of faulting across the western sector of the Market Weighton Block, Vale of York. *Proceedings of the Yorkshire Geological Society* 50, 125 - 128.

Hillis, R. R. 1995. Quantification of Tertiary exhumation in the United Kingdom Southern North-Sea using velocity data. *Aapg Bulletin-American Association of Petroleum Geologists* 79(1), 130-152.

Holland, M. & Urai, J. L. 2010. Evolution of anastomosing crack-seal vein networks in limestones Insight from an exhumed high-pressure cell, Jabal Shams, Oman Mountains. *Journal of Structural Geology* 32(9), 1279-1290.

Kirby, G. A. & Swallow, P. W. 1987. Tectonism and sedimentation in the Flamborough Head region of north-east England. *Proceedings of the Yorkshire Geological Society* 46(4), 301-309.

Knott, S. D., Beach, A., Brockbank, P. J., Brown, J. L., McCallum, J. E. & Welbon, A. I. 1996. Spatial and mechanical controls on normal fault populations. *Journal of Structural Geology* 18(2-3), 359-372.

Lamplugh, G. W. 1895. Notes on the white chalk of Yorkshire. *Proceedings of the Yorkshire Geological Society* 13, 65-87.

Lockner, D. A. & Beeler, N. M. 1999. Premonitory slip and tidal triggering of earthquakes. *Journal of Geophysical Research-Solid Earth* 104(B9), 20133-20151.

Mallon, A. J., Swarbrick, R. E. & Katsube, T. J. 2005. Permeability of fine-grained rocks: New evidence from chalks. *Geology* 33(1), 21-24.

Micarelli, L., Benedicto, A. & Wibberley, C. A. J. 2006a. Structural evolution and permeability of normal fault zones in highly porous carbonate rocks. *Journal of Structural Geology* 28(7), 1214-1227.

Micarelli, L., Moretti, I. & Daniel, J. M. 2003. Structural properties of rift-related normal faults: the case study of the Gulf of Corinth, Greece. *Journal of Geodynamics* 36(1-2), 275-303.

Micarelli, L., Moretti, I., Jaubert, M. & Moulouel, H. 2006b. Fracture analysis in the south-western Corinth rift (Greece) and implications on fault hydraulic behavior. *Tectonophysics* 426(1-2), 31-59.

Milsom, J. & Rawson, P. F. 1989. The Peak Trough – a major control on the geology of the North Yorkshire coast. *Geological Magazine* 126, 699 - 705.

Peacock, D. C. P. & Sanderson, D. J. 1994. Strain and scaling of faults in the chalk at Flamborough Head, U.K. *Journal of Structural Geology* 16(1), 97-107.

Price, M. 1987. Fluid flow in the Chalk of England. *Fluid flow in sedimentary basins and aquifers: Geological society [London] Special Publication*(34), 141-156.

Sagi, D. A., Arnhild, M., Karlo, J. F. 2013. Quantifying fracture density and connectivity of fractured chalk reservoirs from core samples: implications for fluid flow. *Geological Society Special Publications* in Advances in the Study of Fractured Reservoirs. eds: Spence, G. H., Redfern, J., Aguilera, R., Bevan, T. G., Cosgrove, J. W., Couples, G. D. & Daniel, J.-M.. 374

Scholle, P. A. 1977. Chalk diagenesis and its relation to petroleum exploration - Oil from chalks,, a modern miracle. *Aapg Bulletin-American Association of Petroleum Geologists* 61(7), 982-1009.

Seront, B., Wong, T.-F., Caine, J. S., Forster, C. B., Bruhn, R. L. & Fredrich, J. T. 1998. Laboratory characterization of hydromechanical properties of a seismogenic normal fault system. *Journal of Structural Geology* 20(7), 865-881.

Sibson, R. H. 1977. Fault rocks and fault mechanisms. *Journal of the Geological Society* 133(3), 191-213.

Sibson, R. H. 2000. Fluid involvement in normal faulting. *Journal of Geodynamics* 29(3-5), 469-499.

Starmer, I. C. 1995. Deformation of the Upper Cretaceous Chalk at Selwicks Bay, Flamborough Head, Yorkshire: its significance in the structural evolution of north-east England and the North Sea Basin. *Proceedings of the Yorkshire Geological Society* 50, part 3, 213-228.

Stewart, S. A. & Bailey, H. W. 1996. The Flamborough Tertiary outlier, UK southern North sea. *Journal of the Geological Society* 153, 163-173.

Tondi, E. 2007. Nucleation, development and petrophysical properties of faults in carbonate grainstones: Evidence from the San Vito Lo Capo peninsula (Sicily, Italy). *Journal of Structural Geology* 29(4), 614-628.

Wilson, E. J., Friedmann, S. J. & Pollak, M. F. 2007. Research for deployment: Incorporating risk, regulation, and liability for carbon capture and sequestration. *Environmental Science & Technology* 41(17), 5945-5952.

9. Figures

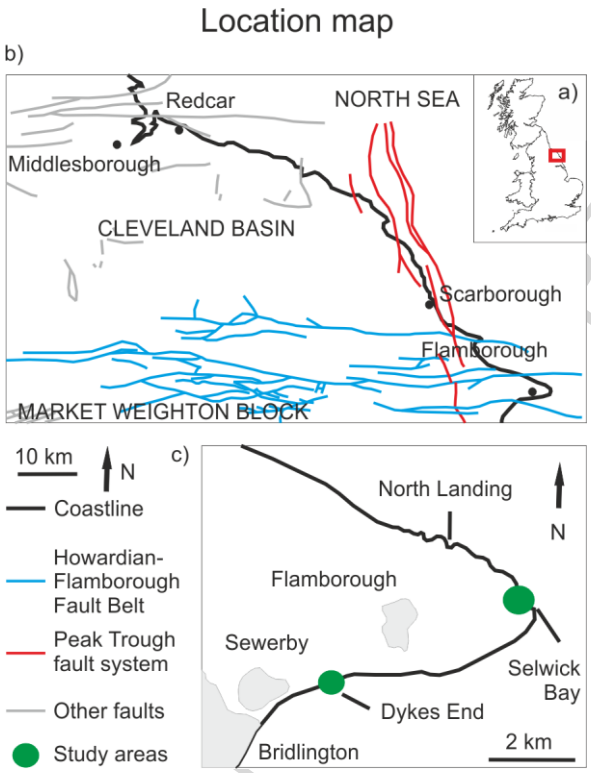

Figure 1: Location map a) outline of the UK with the Flamborough Head area highlighted, b) Location map and geological setting of Flamborough Head, c) study areas (modified after Peacock and Sanderson, 1994)

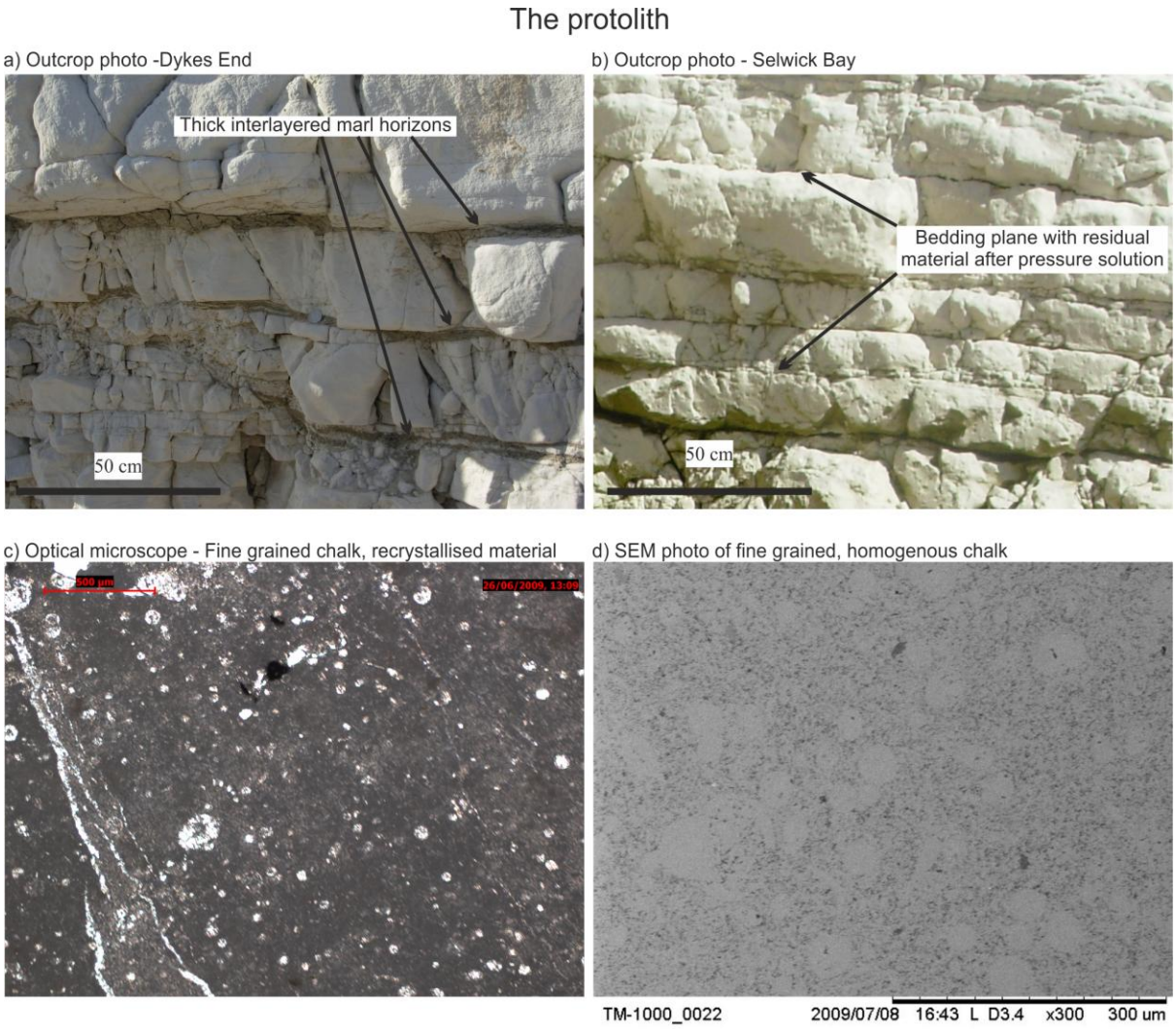

Figure 2: The protolith at a) Dykes End and b) at Selwick Bay: the thickness of the chalk beds varies from a few mm up to 50 cm. Some sub-horizontal, bedding parallel stylolites are present. Bedding surfaces at Dykes End (a) usually contain interlayered marl horizons with a thickness up to 2-3 cm. At Selwick Bay (b) no interlayered marl horizons are present but those bedding planes that are stylolitic surfaces as well contain residual clay material from pressure solution processes, c) Optical microscope photo showing the protolith with examples of recrystallized chalk, d) SEM photo of the fine grained, homogenous chalk

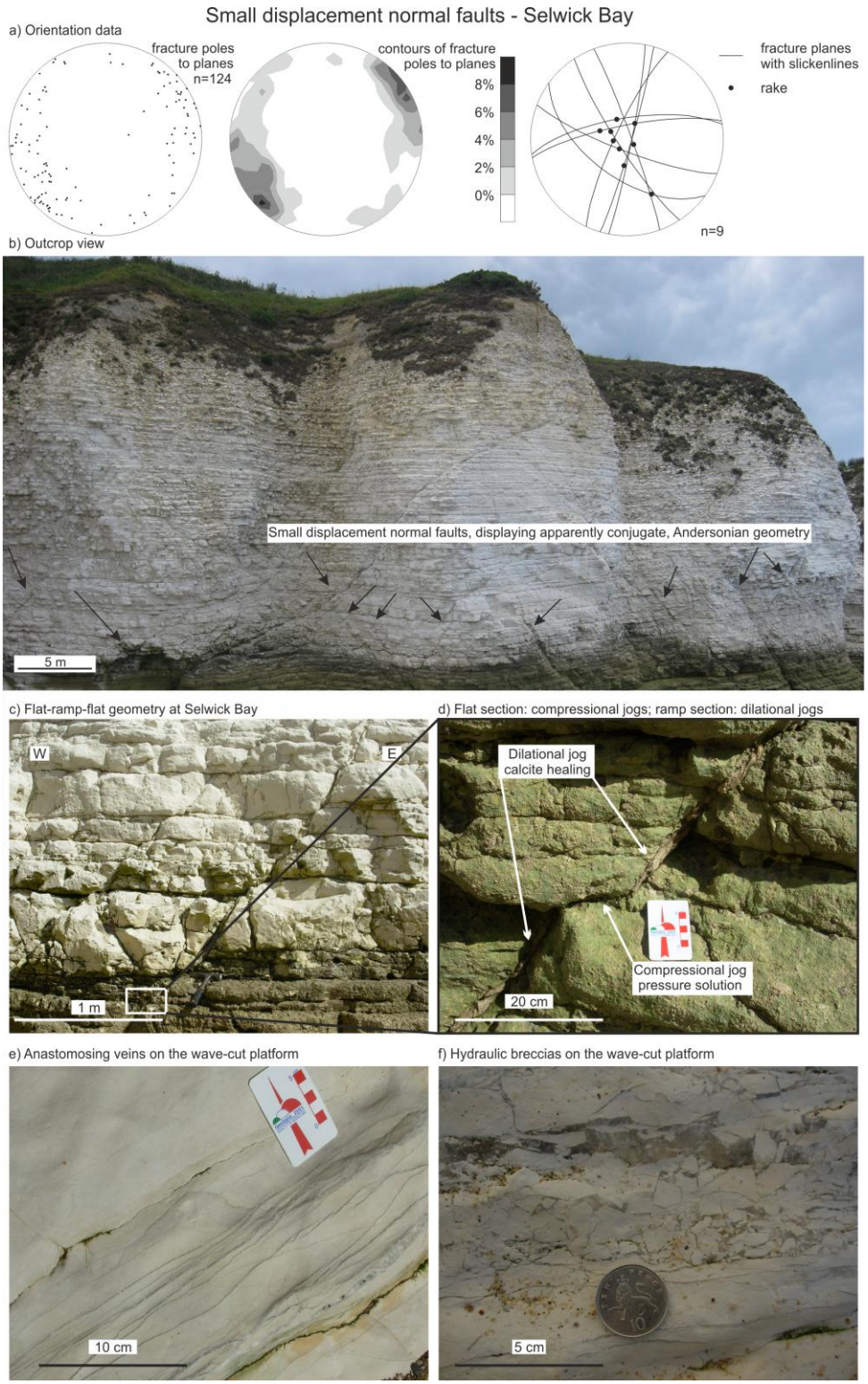

Figure 3: Small displacement normal faults at Selwick Bay a) stereonet of the small displacement normal faults at Selwick Bay with scattered orientation, and one minor NW-SE striking trend, and the slickenline data indicating dip-slip kinematics, b) outcrop view with the most prominent small displacement faults (northern cliff), c) flat-ramp-flat geometry, d) ramp section dilational jogs are healed with calcite veins, while flat section compressional jogs show evidence for pressure solution with some residual material, e) anastomosing veining zone on the wave cut platform indicating crack-seal mechanism, f) vein with

hydraulic brecciation, (notice he increase of damage from the bottom towards the top of the photo)

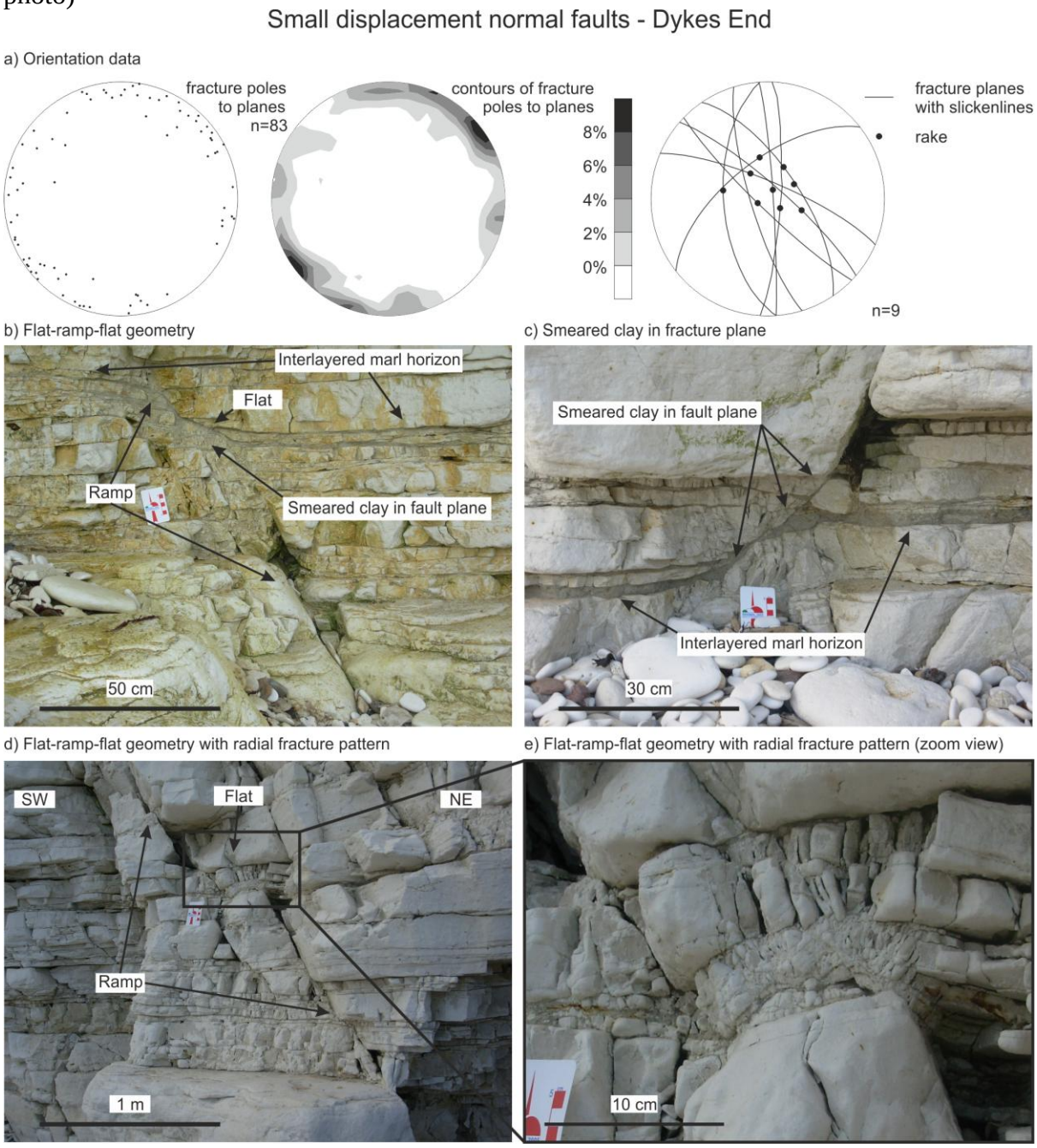

Figure 4: Small displacement normal faults at Dykes End a) stereonet of the small displacement normal faults at Dykes End with scattered orientation, and one minor NW-SE striking trend, and the slickenline data indicating dip-slip kinematics, b) forming flat-ramp-flat geometry while cutting through chalk and interlayered marl horizons, c) smearing of the interlayered marl horizons into the fracture plane, d, e) open fractures organised in a radial pattern around the flat section

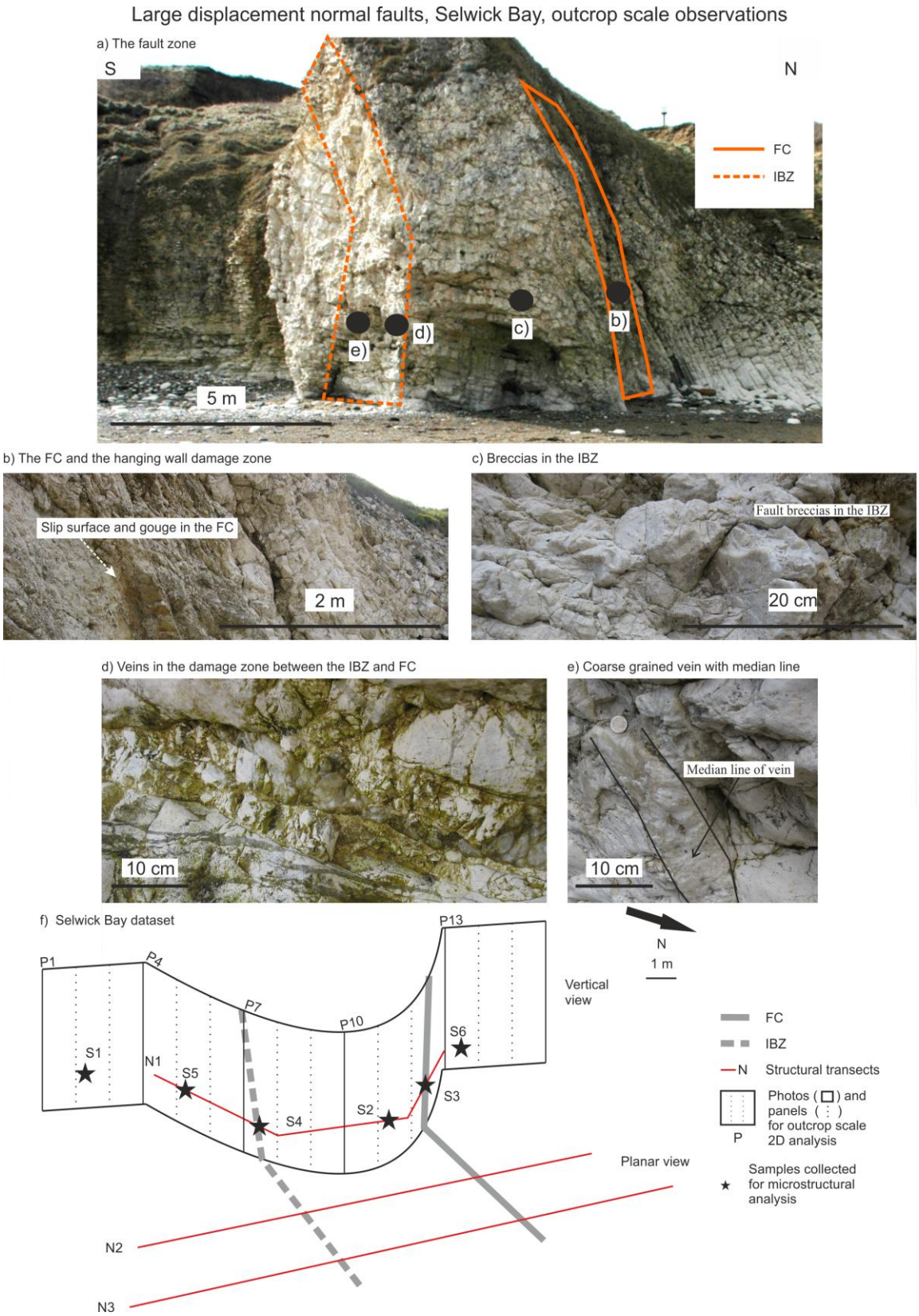

Figure 5: Large displacement normal faults at Selwick Bay – outcrop scale a) the headland forming the fault zone with the FC and IBZ, b) The FC, with a slip surface and sharp contact with the dragged beds of the hanging wall, c) fault breccias in the IBZ, d) thick (> 5 cm) veins with coarse grain crystals cross-cutting braided, narrow veins, e) thick (10 cm) vein with clear median line, f) the 1D and 2D quantitative dataset (transects, photo panels, thin sections) with respect to the location of the large displacement normal faults

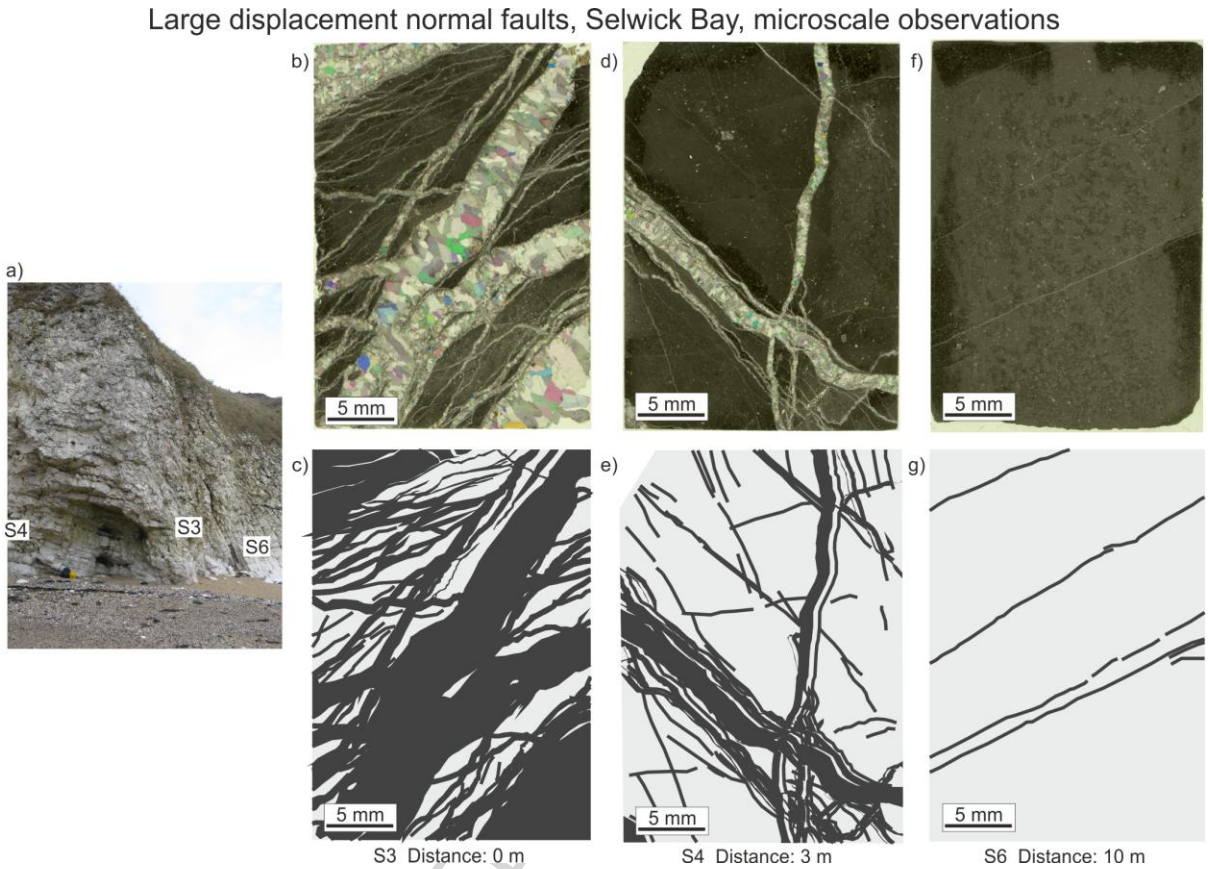

Figure 6: Large displacement normal faults at Selwick Bay – microscale a) original location of the thin sections on the outcrop, b, c) S3 sample from the brecciated part of the FC, showing very high vein density, d, e) S4 sample from the IBZ with intense veining, f, g) S6 sample from the hanging wall protolith with only minor veining

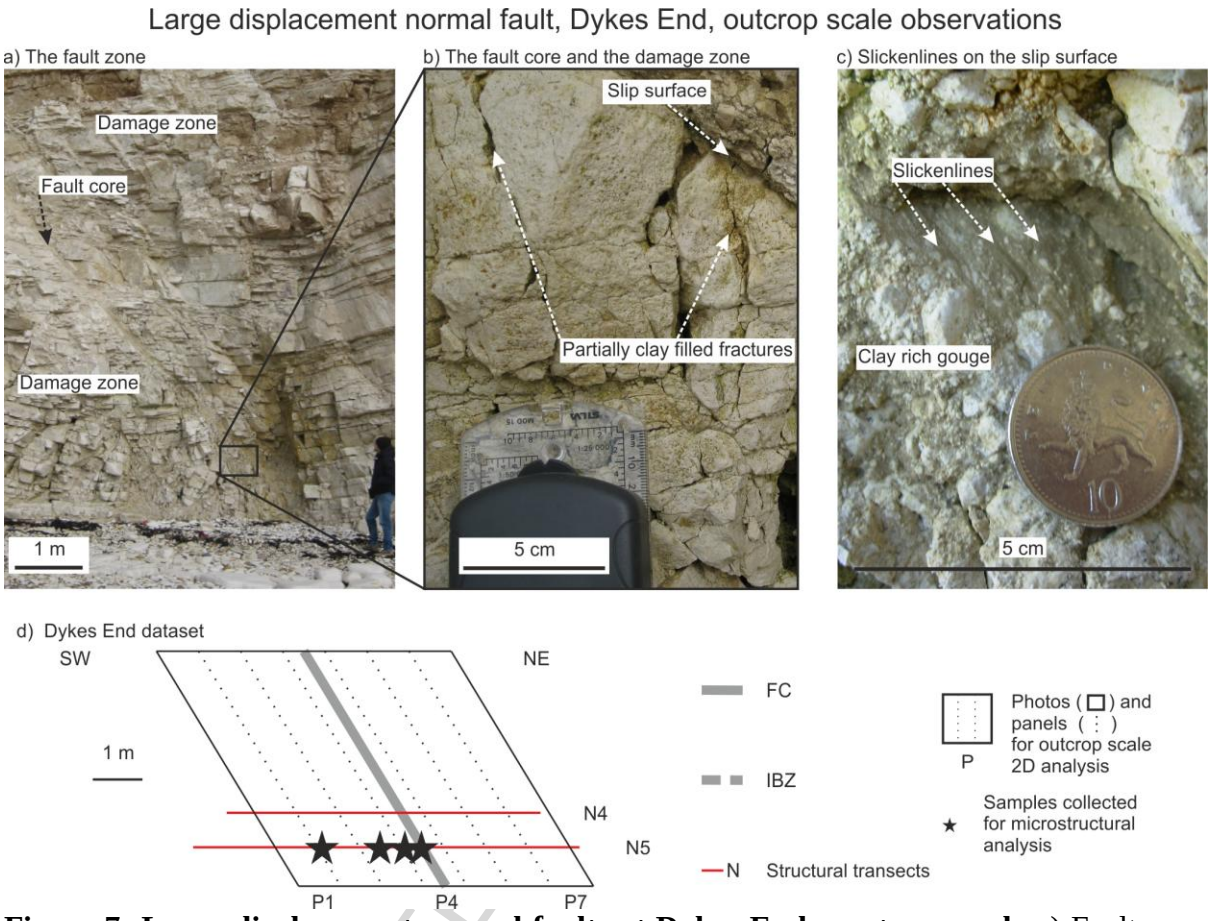

Figure 7: Large displacement normal faults at Dykes End – outcrop scale a) Fault zone with narrow (<20 cm) fault core and surrounding 3-4 m wide damage zone, b) sharp fault core-damage zone boundary, c) slickenlines on the slip surface showing dip slip kinematics, d) the 1D and 2D quantitative dataset (transects, photo panels, thin sections) with respect to the location of the large displacement normal faults

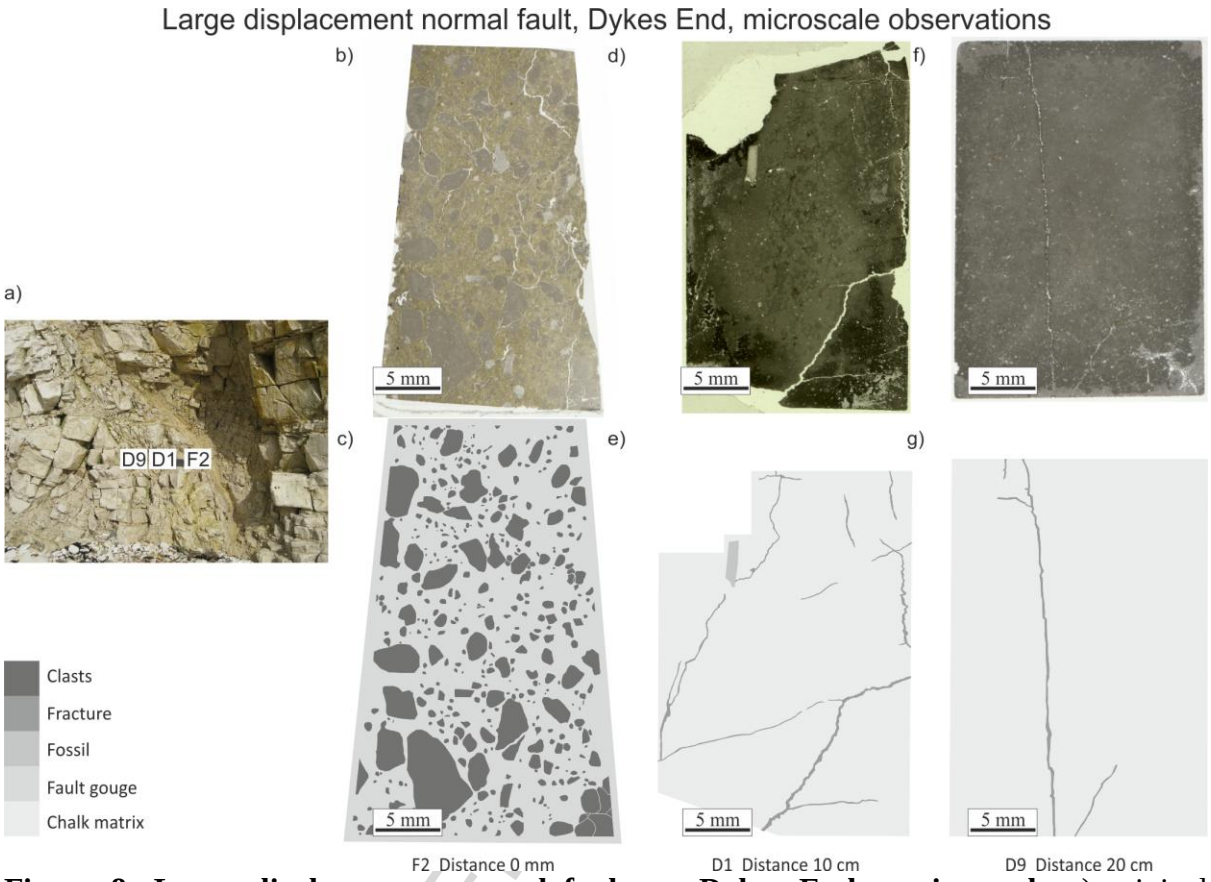

Figure 8: Large displacement normal faults at Dykes End – microscale a) original location of the thin sections on the outcrop: b, c) F2 sample from the fault core, containing fault gouge and some mm-scale clasts of the host rock, d, e) D1 sample, collected 10 cm away from the fault core, containing some fractures that are clay filled due to the injection on the fault plane, and some stylolites, f, g) D9 sample collected 20 cm away from the fault core, showing one clay filled fracture

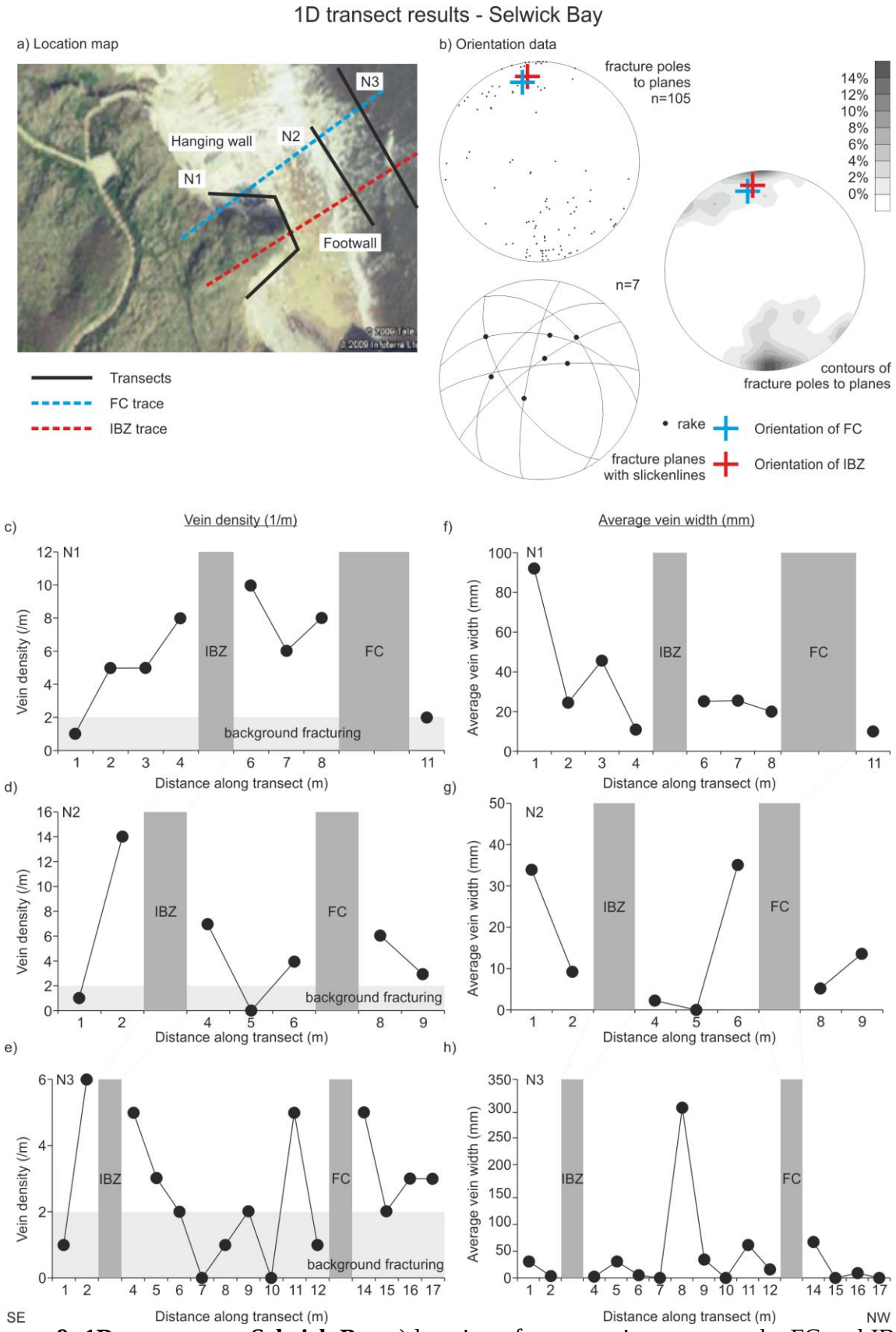

Figure 9: 1D transects at Selwick Bay a) location of transects in respect to the FC and IBZ, b) orientation of veins in the damage zone, and the kinematic indicators on their surfaces, c, d, e) vein density across the fault zone along the three transects, N1-N3, respectively,

f, g, h) average vein widths across the fault zone along the three transects N1-N3, respectively

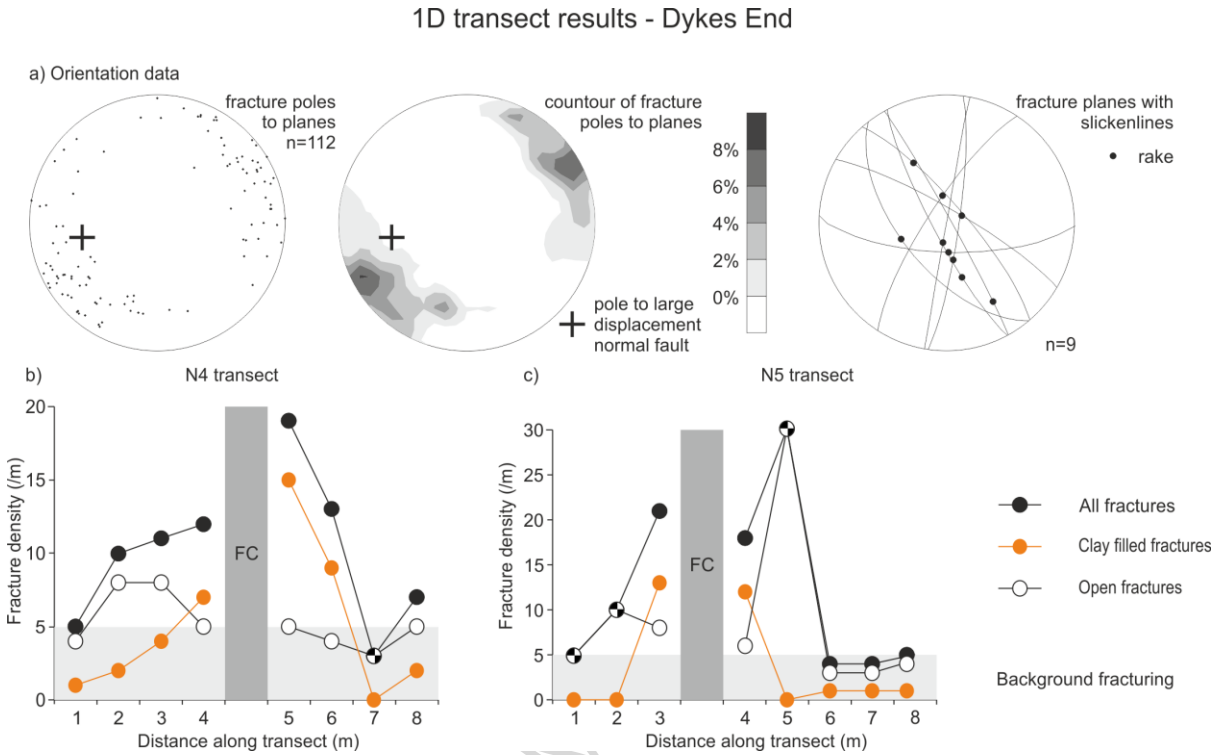

Figure 10: 1D transects at Dykes End a) orientation of the fractures in the damage zone, and the kinematic indicators on their surfaces, b) fracture density across the fault zone and variation in the density of open and clay filled fractures across the fault zone (N4 transect), c) fracture density across the fault zone and variation in the density of open and clay filled fractures across the fault zone (N5 transect); (Note that the fault cores in Fig. 11b-e are represented by a wider zone than its real width, therefore those sections of the graphs are strictly not to scale.)

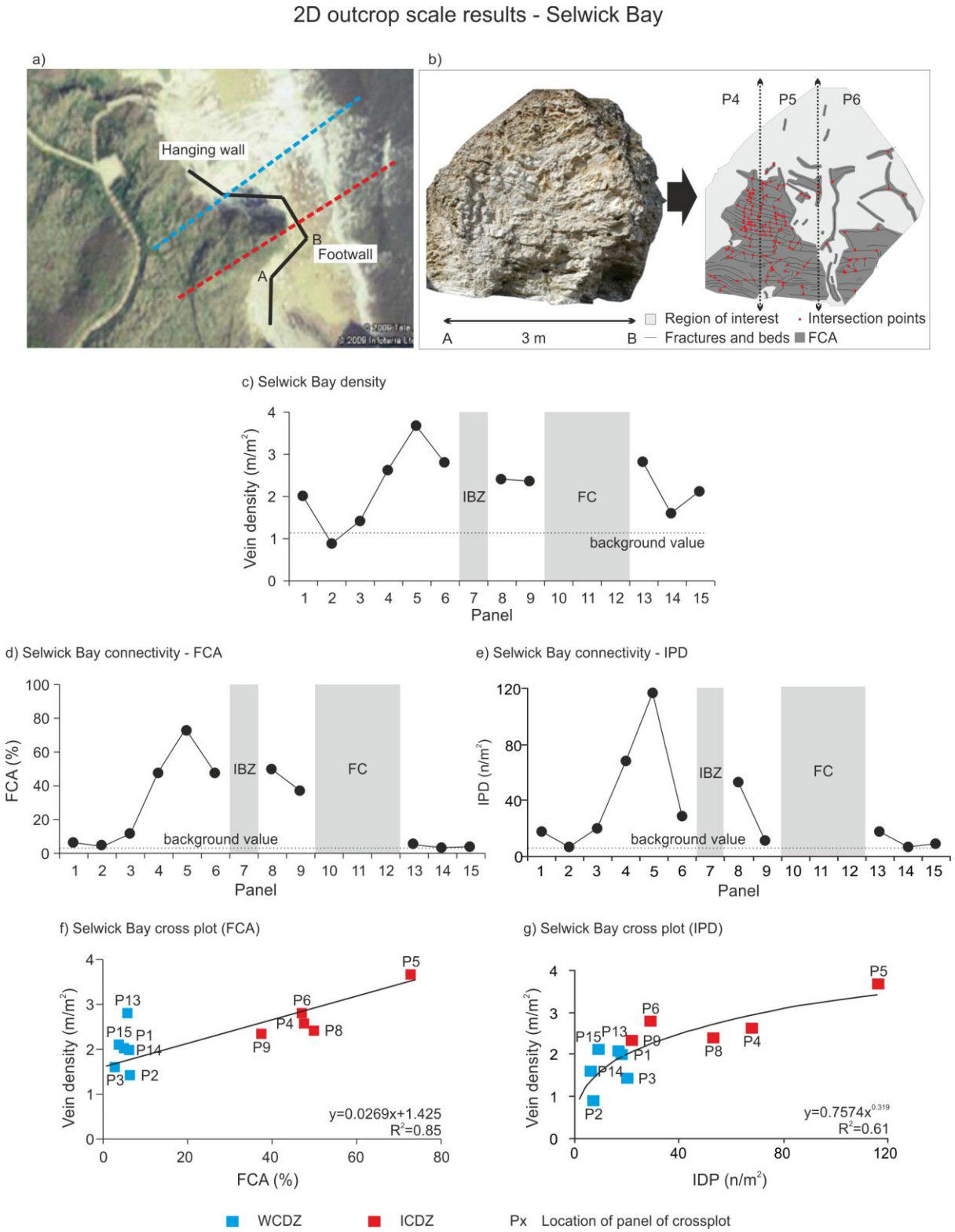

Figure 11: 2D outcrop scale results – Selwick Bay a) Location of photos used for analysis across the headland, b) Example photo showing the panels (P4-P6) used for the analysis with the picked veins, FCA and vein intersection points, c) Changes in vein density along the Selwick Bay large displacement normal faults along all the panels, d) Changes in vein connectivity along the Selwick Bay large displacement normal faults along all the panels (calculated as FCA), e) Changes in vein connectivity along the Selwick Bay large displacement normal faults along all the panels (calculated as IPD), f) Vein density vs.

connectivity crossplot (calculated as FCA), g) Vein density vs. connectivity crossplot (calculated as IPD)

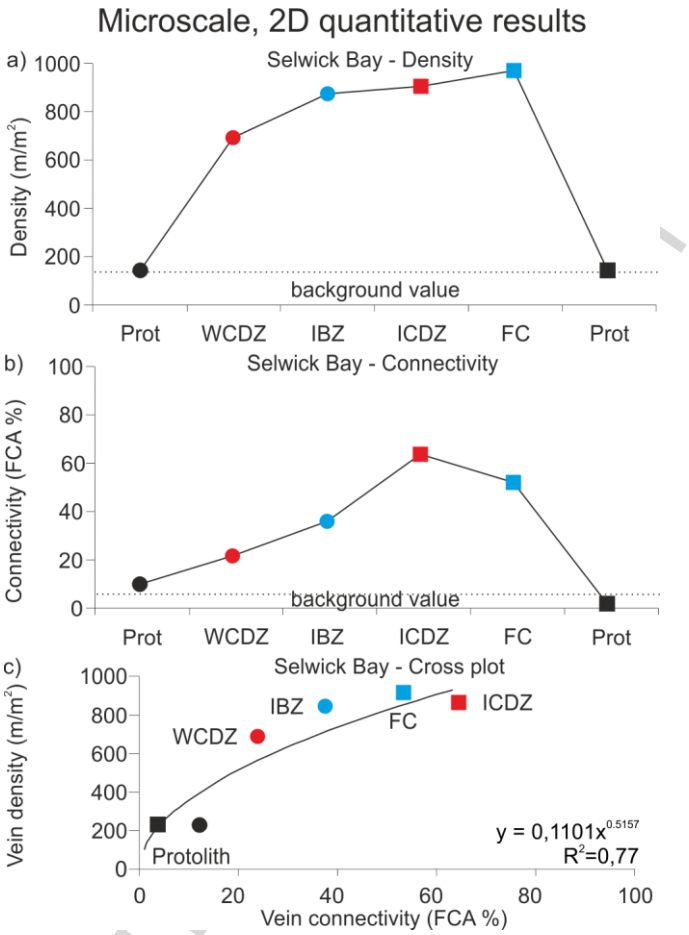

Figure 12: 2D microscale image analysis – Selwick Bay a) Vein density in the different fault zone domains at Selwick Bay, b) Vein connectivity in the different fault zone domains at Selwick Bay, c) Vein density vs. connectivity crossplot of the different fault zone domains at Selwick Bay

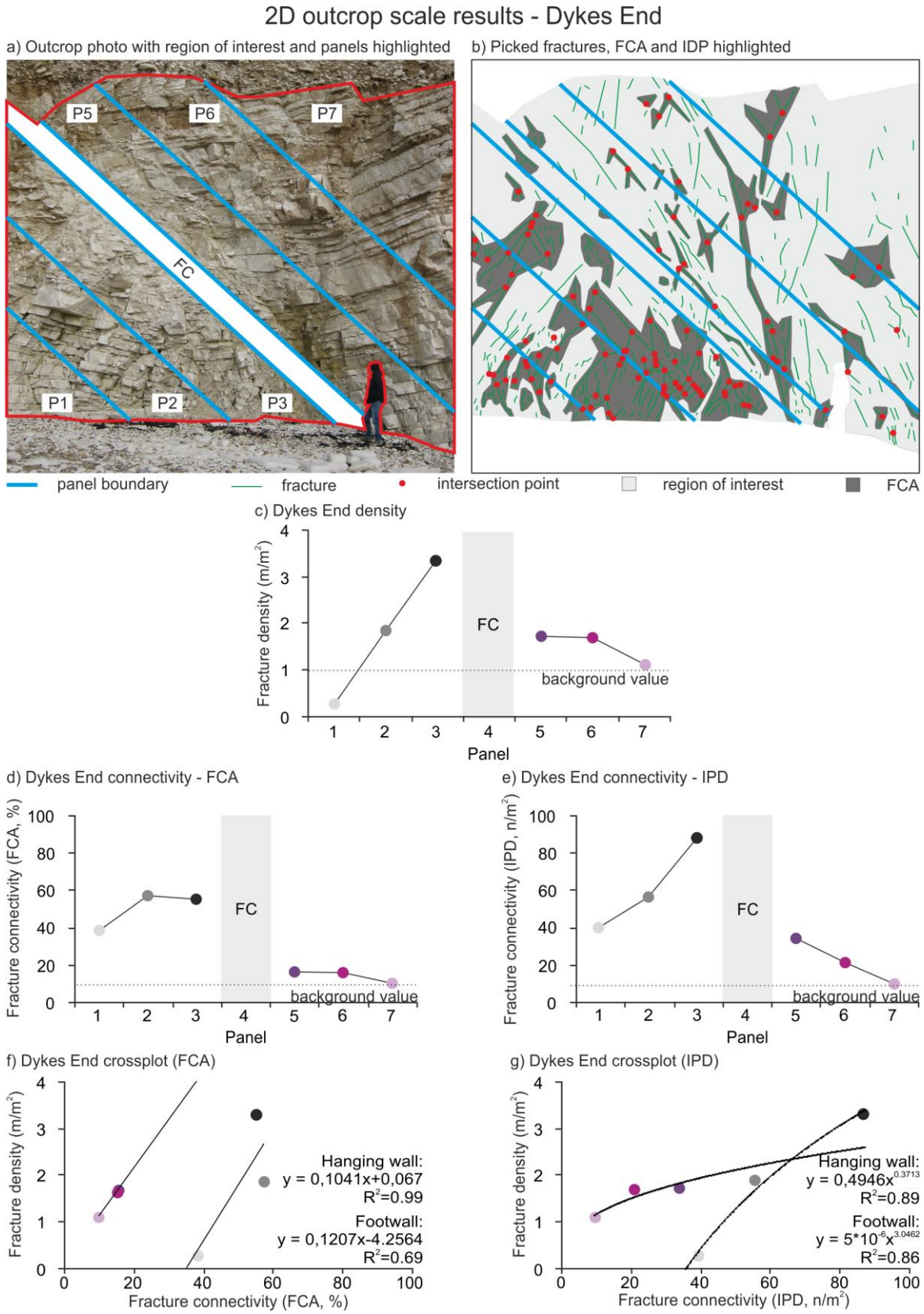

Figure 13: 2D outcrop scale results – Dykes End a) Outcrop photo with the region of interest and panels highlighted, b) Picked fractures with the FCA and intersection points highlighted, c) Fracture density across the fault zone, d) Fracture connectivity across the fault zone (FCA), e) Fracture connectivity across the fault zone (IPD), f) Fracture density vs. connectivity (FCA) crossplot, g) Fracture density vs. connectivity (IPD) crossplot

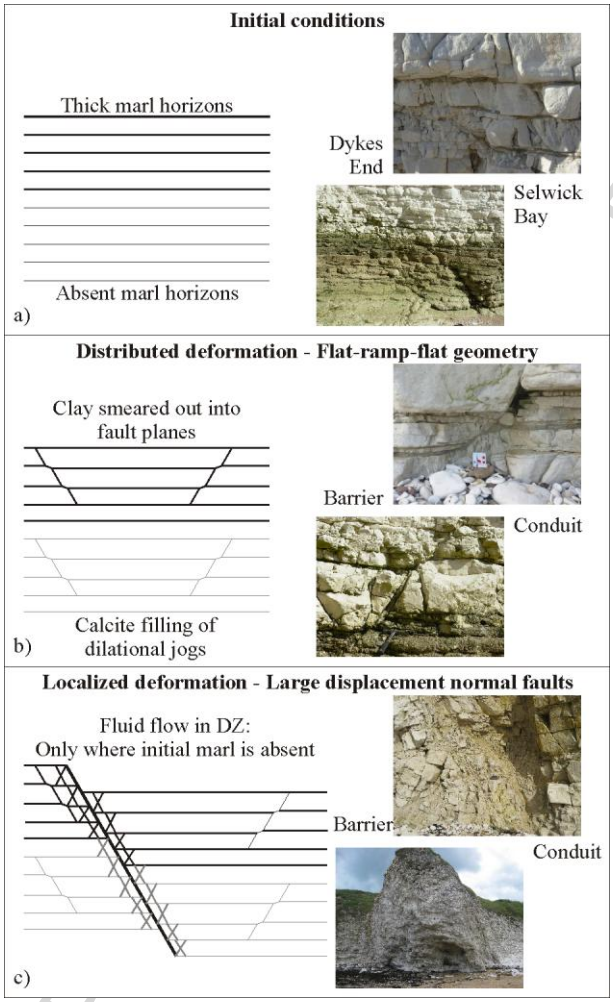

Figure 14: Conceptual model of fault development at Flamborough Head a) initially thick marl horizons deposited within the chalk at Dykes End, and thin to absent marl horizons at Selwick bay, b) distributed deformation developed the small displacement, flat-ramp-flat geometry faults; at Selwick Bay the fractures were healed by calcite as a result of fluid flow, while at Dykes End clay from the interlayered marl horizons were smeared out and injected into the fault planes forming barriers, c) localized deformation developed the large displacement normal faults; at Dykes End the development of the large faults resulted in an even stronger barrier for fluids while at Selwick Bay large faults channelized fluid flow

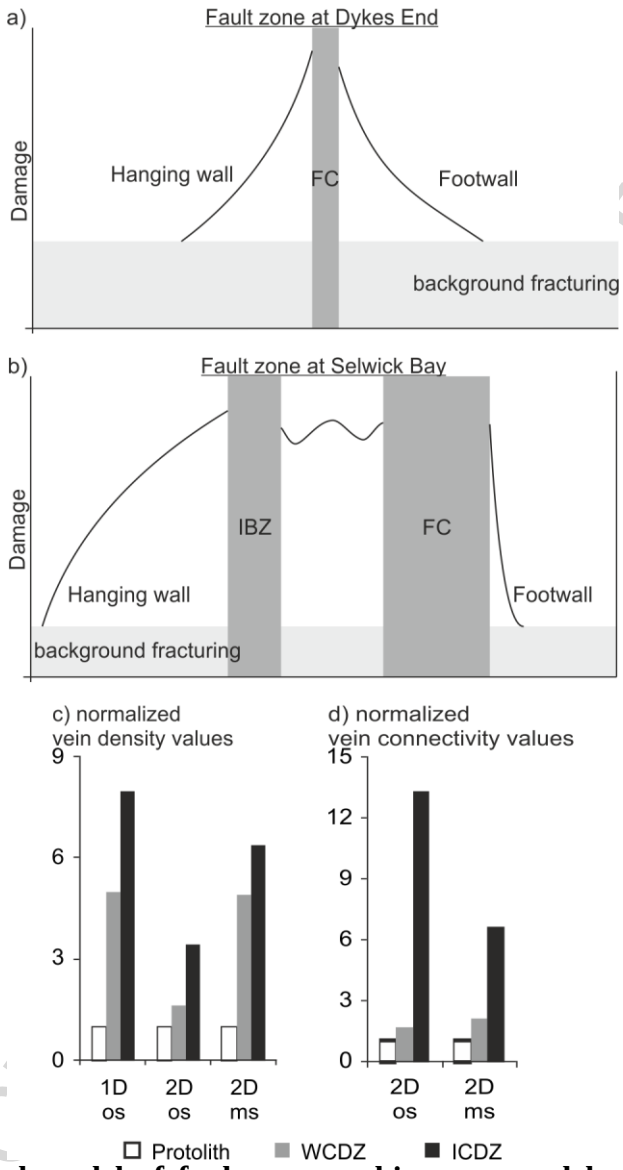

Figure 15: Conceptual model of fault zone architecture model a) at Dykes End, b) at Selwick Bay, c) normalised vein density values at Selwick Bay, d) normalised vein connectivity values at Selwick Bay